

Reactive and harmonic current detection in a nonlinear load with frequency excursions

M. E. Abdel- Karim

Electrical Power and Machines Dept., Faculty of Eng., Tanta Universit, Tanta, Egypt

In this paper, an effective estimator for detecting the reference current of active power filters and Var compensators is presented. The proposed estimator is adaptive and can be used with nonlinear loads under frequency excursions of the power source over a wide range. The effectiveness and accuracy of the proposed method are demonstrated and verified through the presented simulation and experimental results.

تعتبر دوائر القدرة الإلكترونية من أهم مسببات التوافقيات ووجود القدرة الغير فعالة في أنظمة القدرة الكهربائية. ولتعويض التوافقيات والقدرة الغير فعالة للأحمال اللاخطية والمغذاة من مصدر جهد ذي ترددات متباينة ، اقترح هذا البحث مبينا للتيار المرجعي اللازم للتحكم في مرشح قدرة فعال أو معوض إستاتيكي للقدرة الغير فعالة. تم دراسة كيفية إتمام عملية الحصول على التيار المرجعي من تيار حمل لاخطي للطريقة المقترحة. كذلك تم اختبار المبين المقترح معمليا مع محرك تأثيري ثلاثي الأوجه يتم التحكم في سرعته عن طريق دائرة تحكم مغلقة لمجموعة مكثفات متصلة بعضوه الدوار. وقد أظهرت النتائج قدرة المبين على استنباط التغيرات في التيار الغير فعال والتوافقيات مع عدم تأثر المركبة الفعالة لتيار المحرك عند تغيير سعة المكثفات فقط وثبوت كل من سرعة المحرك والحمل. وتبين النتائج قدرة المبين على قياس أي مركبة من مركبات تيار الحمل عند الحاجة لذلك.

Keywords: Active filters, Adaptive filters, Harmonic elimination, Reactive power compensation

1. Introduction

The increased use of power converters, adjustable speed drives, electronic devices, and non-linear loads, contribute to excessive harmonic distortion in power systems. As a consequence, compensation of reactive and harmonic currents becomes more and more important.

So far, passive filters have been used for this purpose, however they have limitations to be overcome. Active filters and static Var compensators have been developed in recent years, but they require measuring systems with high accuracy and rapid detection for reactive and harmonic currents. Active power filters have been developed, such as the shunt active filter shown in fig. 1 [1].

Several methods have been proposed for detecting harmonic and/or reactive currents. Conventionally, analog notch or band pass filters are used to extract harmonics in power system control. Recently, a control method based on real-time digital simulation of an LC filter for each harmonic accomplished by a DSP have been proposed. To adjust the harmonic current compensation in distribution lines via an active filter, adaptive

gain controller has been used [2]. A drawback of these filters is that the corner frequency is sensitive to parameter variations of the elements and the filtering process will be worse as the ac source frequency fluctuates. To avoid this problem, an adaptive band-pass filter has been proposed to detect the harmonics current with wide range variations of ac source frequency [3, 4].

Reactive and harmonic current reference can be determined in many different ways. Usually, integrative methods such as fast integration method [5], least compensation current method [6], Fryze's time domain analysis [7], and Fourier analysis [1,7,8] are applied, resulting in good steady state and moderate response of consequent line current to the load current change. Fast Fourier Transform (FFT) method needs two FFT transformations that take about 31ms to complete [7,8]. In addition, a distorted voltage will cause a non-synchronous sampling error. However, a detecting method based on instantaneous reactive power theory [9] and instantaneous active and reactive power p-q method [10] are only suitable for a three-phase system. In implementation, these methods need several high accuracy

multipliers. So their features are complicated in structure, difficult to adjust, and poor in performance. A multistage adaptive filtering system has been proposed to extract the sinusoidal active current from the distorted waveform without harmful phase shift even when the frequency and amplitude alter simultaneously [11]. However, due to the complexity of the model, the study has been restricted to simulation. A compensator using control logic circuits operated in cycle-cycle reference current controlled has been proposed to compensate the reactive and harmonic current [12]. The main disadvantage of this method is that the amplitude of the supply current reference remains constant between all zero-crossing instants of the source voltage.

In addition to the above mentioned shortcomings, the methods are affected by voltage distortion, since their detecting systems are open loop which are sensitive to component parameters variations and operating conditions. These directly affect the measuring accuracy. Two closed loop detection methods were proposed [7, 13]. In

reference [7], an analog detection method based on adaptive interference canceling theory depending on the least squares algorithms is proposed to minimize the error signal between the actual and detected compensating current. In addition to the well-known problems of using analog components, the shortcoming of this method is that it needs mathematical tools to ensure the optimal minimum error. Reference [13] uses a digital low-pass filter with fixed parameters to detect a reactive and harmonic current reference for a limited range of source frequency variations on the expense of degradation of the filter performance.

This paper presents a new closed-loop and instantaneous adaptive estimator based on adaptive band-pass digital filter for detecting the reactive and harmonic current reference in a non-linear load under frequency excursions of the power source over a wide range. The corresponding detection system is developed. Simulation and experimental results are given, which verify that the proposed estimator overcomes the shortcomings of the methods mentioned above.

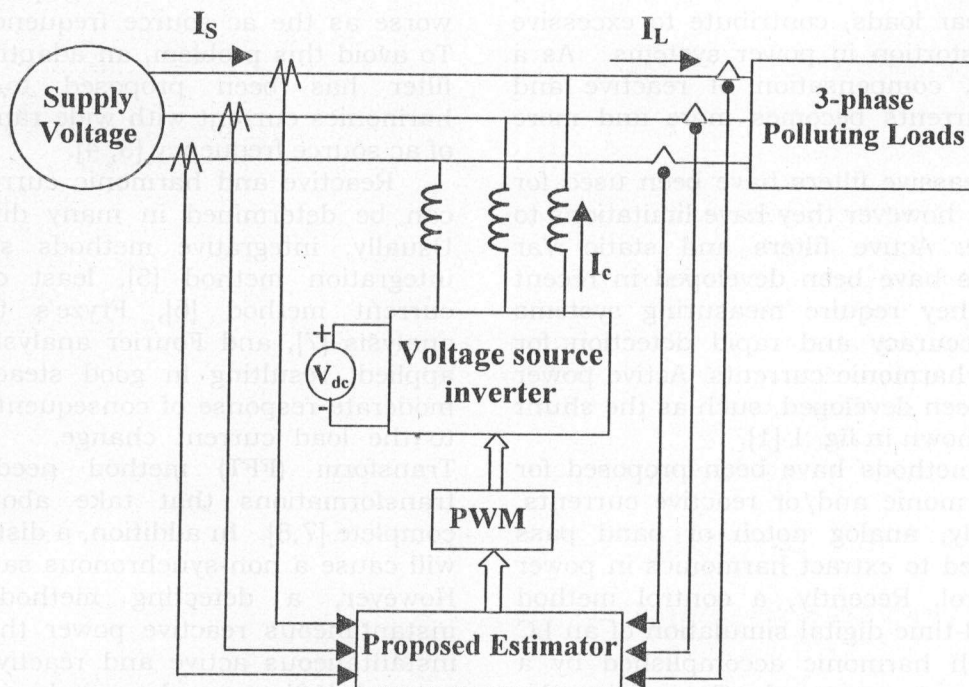


Fig. 1. Voltage source inverter as a shunt filter.

2. The proposed estimator

2.1. Basic principle

For supply voltage v_s is given by;

$$v_s = \sqrt{2}V_s \cos \omega t. \quad (1)$$

The non-linear load current in a power system, in general, is made up of the following terms:

$$i_L(t) = i_{L0}(t) + i_{Lp}(t) + i_{Lq}(t) + i_{Lh}(t), \quad (2)$$

where:

i_{L0} is the dc component,

i_{Lp} is the active current (in-phase line current),

i_{Lq} is the reactive current,

i_{Lh} is the harmonic current.

Eq. (2) can be further expanded in the general form [12];

$$i_L(t) = I_{L0} + I_{Lp} \cos \omega t + I_{Lq} \sin \omega t + \sum_{j=1}^{\infty} I_{L2j} \cos(2j\omega t + \Phi_{2j}) + \sum_{k=1}^{\infty} I_{L(2k+1)} \cos((2k+1)\omega t + \Phi_{2k+1}). \quad (3)$$

The first and second summations represent the even and odd harmonics. The only component that the mains should supply, is the active current i_{Lp} . It can be noted that, the active filter supplies the compensation current (i_c) that contains the dc component, the reactive, and harmonic currents for the load. Then, the main needs only to supply the active current. This can be easily accomplished by subtracting the active current component i_{Lp} from the load current i_L ,

$$i_c(t) = i_L(t) - i_{Lp}(t) = i_L(t) - I_{Lp} \cos \omega t. \quad (4)$$

By multiplying both sides of eq. (3) by $\cos \omega t$;

$$i_L(t) \cos(\omega t) = I_{L0} \cos(\omega t) + 0.5I_{Lp}[1 + \cos 2\omega t] + 0.5I_{Lq} \sin 2\omega t + \sum_{j=1}^{\infty} \frac{I_{L2j}}{2} [\cos((2j+1)\omega t + \Phi_{2j}) + \cos((2j-1)\omega t + \Phi_{2j})] + \sum_{k=1}^{\infty} \frac{I_{L(2k+1)}}{2} [\cos((2k+2)\omega t + \Phi_{2k+1}) + \cos(2k\omega t + \Phi_{2k+1})]. \quad (5)$$

If a band pass filter whose center frequency is at 2ω and its input is as given by eq. (5), the filter output becomes:

$$\Delta i_{ep}(t) = 0.5 I_{Lp} \cos 2\omega t + 0.5 I_{Lq} \sin 2\omega t. \quad (6)$$

This output is treated to obtain i_c in a compensating current estimator circuit by adding a feedback loop and an integral gain block as shown in fig. 2.

2.2. General description of the estimator

To analyze the estimator circuit shown in fig. 2, assume it has reached a steady state condition, since the integrator forces its average input Δi_{ep} to zero. With this condition, the integrator output I_{ep} becomes a dc. If this dc value is multiplied by $\sin \omega t$ or $\cos \omega t$, the closed loop modifies the integrator output to the peak value of the reactive or active current component, respectively. In the case of multiplying this dc value by a $\cos \omega t$ as shown in fig. 2, the multiplier output becomes;

$$i_{ep}(t) = I_{ep} \cos \omega t.$$

At the summing node, after the subtraction takes place, the feedback signal to the active current estimator block becomes;

$$i_c(t) = i_L(t) - i_{ep}(t) = i_L(t) - I_{ep} \cos \omega t. \quad (7)$$

After multiplication with in-phase sinusoid, eq. (7) becomes;

$$i_c(t) \cos \omega t = i_L(t) \cos \omega t - I_{ep} \cos \omega t \cos \omega t$$

$$= i_L(t) \cos \omega t - 0.5 I_{ep} (1 + \cos 2\omega t). \quad (8)$$

The multiplication output enters the band-pass filter and the output due to the first term of eq. (8) is eq. (6). The band-pass will eliminate the dc component (-0.5 I_{ep}) in the second term of eq. (8), and will pass -0.5 I_{ep} cos2ωt. Then, the total filter output is;

$$\Delta i_{ep} = 0.5 I_{Lp} \cos 2\omega t - 0.5 I_{ep} \cos 2\omega t + 0.5 I_{Lq} \sin 2\omega t. \quad (9)$$

The average of the reactive current, the third term in eq. (9), during one quadrant cycle becomes zero. Beside, the integrator forces the second term to equal the first term, i.e. I_{ep} equal to I_{Lp}. In this form, the estimated active current i_{ep}(t) is an accurate representation of the in-phase actual active current i_{Lp}(t) in the power circuit. In this case, the estimator output i_c(t), eq. (7), represents the actual compensating current that contains the dc component, the reactive and harmonic currents for the load.

The proposed estimator requires a low-distortion sinusoid with good phase tracking with respect to the supply voltage. To get this clean in-phase sinusoid (cosωt), a digital phase-locked loop (DPLL) is used as shown in fig. 2. However, its amplitude is not relevant.

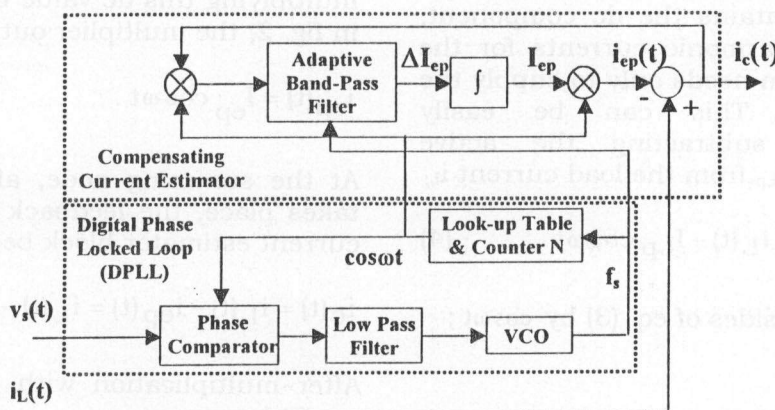


Fig. 2. Closed-loop diagram for estimating the compensating current.

2. 2. 1. Adaptive band-pass filter

The adaptive band-pass filter is necessary to extract the second harmonic current signal filtering from i_c(t) cosωt as shown in fig. 2, especially for the frequency variations of supply voltage. This current signal is filtered by a digital infinite impulse response (IIR) band-pass filter whose transfer function in z-domain is:

$$G(z) = \frac{\beta_0(1 - 2z^2 - z^4)}{1 + \alpha_1z + \alpha_2z^2 + \alpha_3z^3 + \alpha_4z^4}, \quad (10)$$

where, the filter coefficients are listed in the appendix.

This digital filter is transformed from the normalized analog second order Butterworth low-pass filter [14, 15]:

$$G(s) = \frac{1}{1 + \sqrt{2}s + s^2},$$

where;

$$s = \frac{1 - 2 \cos(\omega_0 T_s)z + z^2}{z^2 - 1}.$$

The filter coefficients are determined for sampling frequency f_s (1/T_s) and a center frequency f₀, which must be equal to the frequency 2f₁ of the fundamental supply voltage, as stated above. However, the

frequency variations of the supply voltage need to adjust the filter parameters to twice the frequency of the fundamental. This method involves so many computations, in addition, the value of this frequency must be known which is not an easy task. So, in order to force the center frequency of the filter to follow the input frequency without changing its coefficients, the sampling frequency f_s must be proportional with fundamental frequency f_1 by a frequency multiplier N , i.e. $f_s = Nf_1$ [3]. With this condition, and by putting,

$$z = e^{j\omega T_s} = e^{j2\pi f_1 / f_s} = e^{j2\pi / N},$$

eq. (10) becomes;

$$G(z) = \frac{\beta_0(1 - 2e^{j4\pi/N} - e^{j8\pi/N})}{1 + \alpha_1 e^{j2\pi/N} + \alpha_2 e^{j4\pi/N} + \alpha_3 e^{j6\pi/N} + \alpha_4 e^{j8\pi/N}} \quad (11)$$

It can be noticed from eq. (11) that, the filter characteristics (magnitude and phase) do not change with the frequency variations. Keeping the ratio between f_s and f_1 constant, a counter N is added to the DPLL as shown in fig. 2.

2. 2. 2. Digital phase-locked loop

The concept of digital phase-locked loop (DPLL) is used to implement the supply voltage in-phase sinusoidal generator and the counter N as shown in fig. 2 [16]. This permits one to obtain zero phase error under steady state over a wide range of input frequencies, restricted only by the band width of the low-pass filter and the control range of the sinusoidal voltage controlled oscillator. The exact phase tracking with respect to the input is ensured by the integrator of the low-pass filter $(1+T_1s)/T_2s$. The linear interpolation technique is used to generate an accurate $\cos \omega t$, with a minimum harmonic distortion, from a look-up table with the adaptive sampling frequency $f_s (=Nf_1)$. In this look-up table, sine values for N angles, which are uniformly spaced around the unit circle, are stored. The DPLL accepts a square wave as an input, the ideal transducer for this circuit is a fast electronic transducer (40 μ s) of type (LV25

from LEM), which provides a galvanic isolation, and a good tracking with respect to the supply voltage.

3. Simulation and experimental results

3.1. Parameters election

The parameters for the integrator and the band-pass filter were adjusted empirically by means of computer simulation for a 50Hz system. A suitable time constant for the integrator was found to be 0.0007 sec. The center frequency of the band-pass filter was adjusted to $f_0=100$ Hz, as stated in section 2, with bandwidth=12Hz, and sampling frequency f_s is 5KHz, i.e. $T_s=0.0002$ sec. According to these values and from the appendix, the filter parameters are $\alpha_1 = -3.754$, $\alpha_2 = 5.473$, $\alpha_3 = -3.658$, $\alpha_4 = 0.949$, and $\beta = 0.00033$. With these parameters and taking

$z = e^{j\omega T_s}$ in eq. (10), the filter magnitude and phase characteristics at the center frequency, i.e. $\omega=2\pi(100 \text{ Hz})$, are 1 and 0° , respectively. The attenuation and phase at $\omega=2\pi(50 \text{ Hz})$, are -32.76 dB, and 12.38° . Also, the attenuation and phase at $\omega=2\pi(150 \text{ Hz})$ are -32.88 dB, and -12.29° . However, one comes to the conclusion that only the second harmonic present in eq. (8) to generate eq. (9) at the output of the band-pass filter and the other components are likely to be small or not present at all. According to eq. (11) and for a constant value of frequency multiplier (N was taken 100), the above filter characteristics do not change with the supply frequency variations.

The DPLL was adjusted in order to operate properly in the range of frequencies from 15 to 100Hz, however, a larger frequency operating range is possible.

3. 2. Evaluation

For evaluating the efficiency of the proposed estimator, a very distorted waveform is constructed, as shown in fig. 3-a. The fundamental component of the test signal varies from 40Hz at the sweeping rate of 80Hz/sec. This fundamental component was resolved into its two active and reactive components. The active component is taken

as a fixed component, while the magnitude of the reactive component was suddenly changed by 1.5 times. Besides, the test signal contains an offset current and several low-order harmonics up to the 9th component. Accordingly, for the supply voltage reference v_s , given by eq. (1), and load current is:

$$i_L = 0.25 + 3 \cos xt + 0.5a \sin xt + \frac{a}{3} \cos(3xt + 0.3) + \frac{a}{5} \cos 5xt + \frac{a}{7} \cos 7xt + \frac{a}{9} \cos 9xt, \quad (12)$$

where:

x is the $2\pi 50 + rt$,

a varies from 1.5 to 3 at 0.47 second,

r is the rate of freq. variation, 80Hz/sec.

When the test signals, eqs. (1, 12), are applied to the proposed estimator shown in fig. 2, the simulation results of fig. 3 (left) clearly show that the proposed estimator very well tracks with the amplitude and ramp frequency variations of the load current shown in fig. 3-a. The compensating current reference $i_c(t)$ is illustrated in fig. 3-b. Fig 3-c illustrates the estimated active current along with ideal active current (term 2 in eq. (12)). As mentioned above, this estimated active current remains unchanged and is nearly locked in-phase and in magnitude with ideal active current and in-phase with the supply voltage reference (fig. 3-d). From fig. 3-c, it can be observed, that reactive and harmonic components would be effectively attenuated if the compensating current i_c of fig. 3-b was scaled and injected into the power system in fig. 1. Fig. 3-e illustrates the band-pass filter output with a frequency of twice the fundamental. fig. 3-f shows the integrator output with constant average value as expected from eq. (12) and fig. 3-c. These figures ensure the behaviour of the proposed estimator that has been derived in section 2.

3. 3. Implementation

The software was implemented in LabView and C. The routines that perform the compensating current estimator in real time are implemented in C. The execution of these routines is fired periodically by the computer timer routines. The estimator routines sample the external signals and use the parameters

defined in the parameters buffer to calculate the compensating current (i_c). Some of the signals are stored in the signals buffer allowing the LabView virtual instruments (VI's) to monitor them.

The LabView VI's work as a graphic user interface that allows one to start the estimator, define the reference signals, change the parameters of the estimator, and monitor the signals through charts and graphs.

These VI's are linked to the external C routines, which run in the background in real time. The communication between the external C routines and the LabView VI's is accomplished through some VI's that read from the buffers using code interface nodes (CINS). While, the C routines acquire the data from the data acquisition card, Lab-pc1200 using NI-DAQ driver software.

3. 4. Application

Fig. 4 shows the proposed estimator implemented with a speed controlled wound-rotor induction motor driving a constant mechanical load torque. The motor generates reactive and harmonic currents due to the employment of a PWM transistor-controlled capacitive network in the rotor circuit with a fixed carrier frequency [17]. The reactive and harmonic stator currents can be adjusted by varying the capacitor network. The constant mechanical load is implemented by using a closed loop current control through a PI controller and a half-controlled thyristor bridge with constant current reference for a separately excited DC machine. The parameters of the induction motor and the dc machine are listed in appendix.

In order to have a fixed stator active current, the mechanical load torque is fixed at constant speed of induction motor. This can be achieved at constant current reference for dc machine and at constant speed reference for induction motor. Under these conditions, and at capacitor per phase of $11\mu\text{F}$, the stator currents have fixed values of harmonics, active, and reactive components as shown in fig. 5. Then, each rotor capacitor was suddenly increased to $20\mu\text{F}$ to have reactive and harmonic currents step change in the stator currents. After this, the estimated

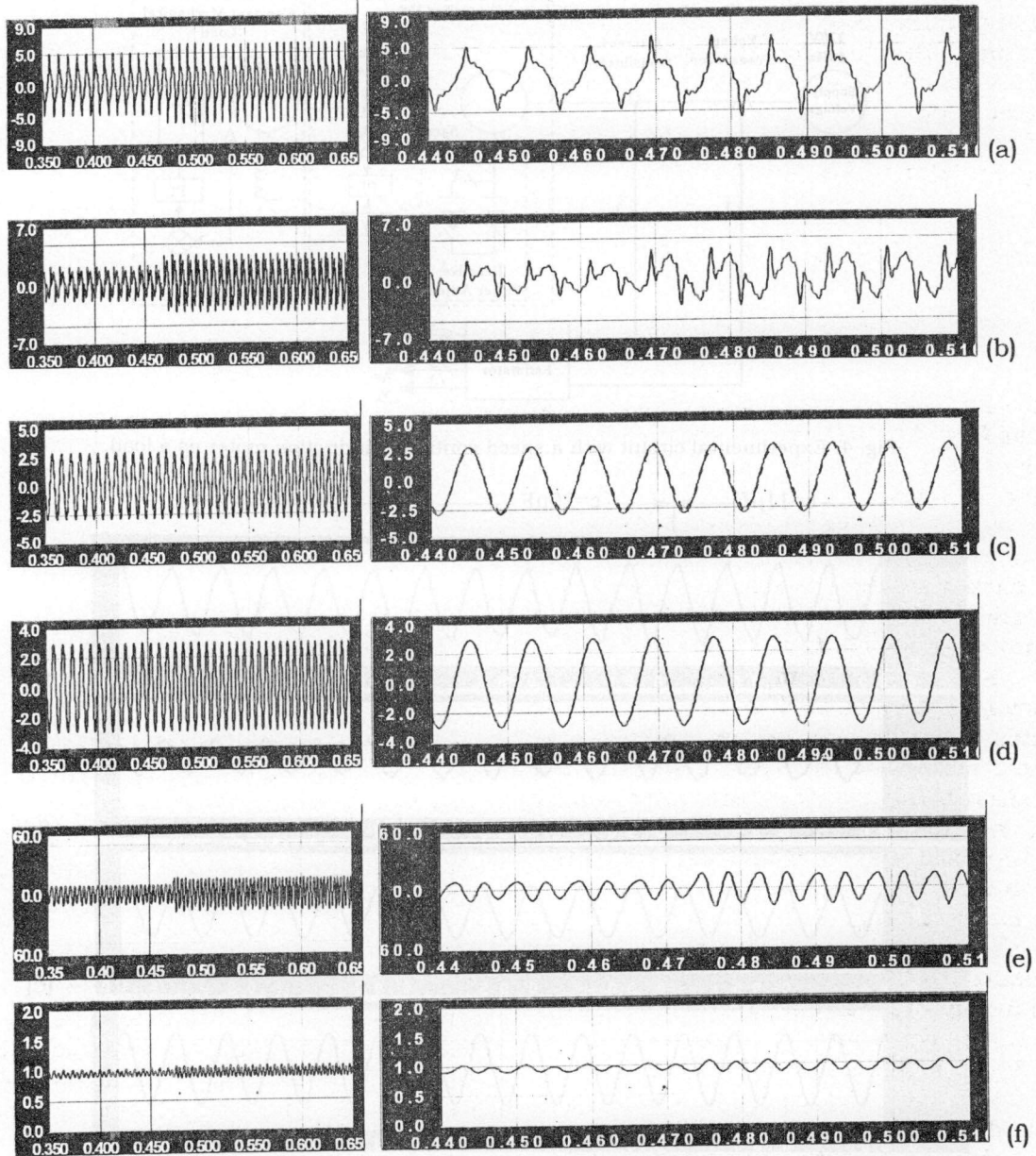


Fig.3. Simulation with a distortion wave signals (eqs. (1) and (12)) with amplitude and frequency variations. a- Load current, i_L . b- Estimated compensating current, i_c . c- Solid line: ideal active current, i_{ip} ; dashed line: estimated active current, i_{ep} . d- Supply voltage reference, v_s . e- Band-pass filter output, Δi_p . f- Integrator output, I_p . (At right, zoomed portion between 0.44 and 0.51sec)

active current remains unchanged and no significant perturbation is introduced by reactive and harmonics current step change in stator currents as shown in fig. 5-c. In fig. 5, trace (a) is the stator current, $i_L(t)$, trace (b) is the estimated compensating current which contains high frequency ripples, harmonics, sub-harmonics, and reactive currents produced in the stator current, $i_c(t)$. Trace (c)

is the estimated active current, $i_p(t)$, and trace (d) is the reference supply voltage, v_s , trace (e) is the output of the band-pass filter, $\Delta i_p(t)$, with a frequency of twice the fundamental frequency. Trace (f) is the motor speed and the integrator output, I_p with constant average value. These figures verify the behaviour of the proposed estimator as expected in section 2.

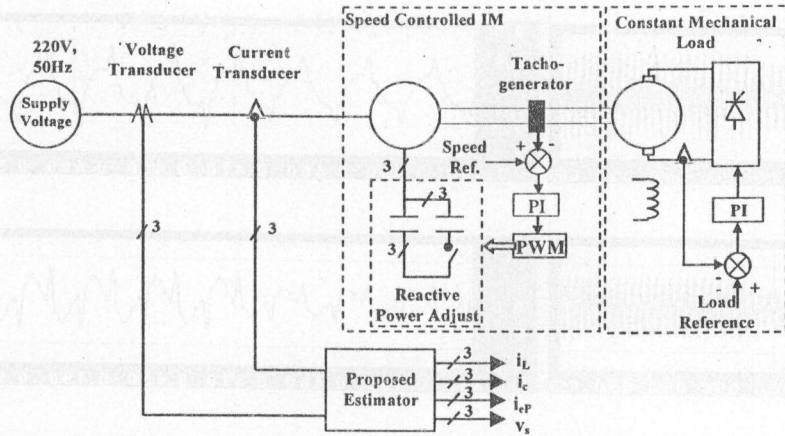


Fig. 4. Experimental circuit with a speed controlled induction motor as a load.

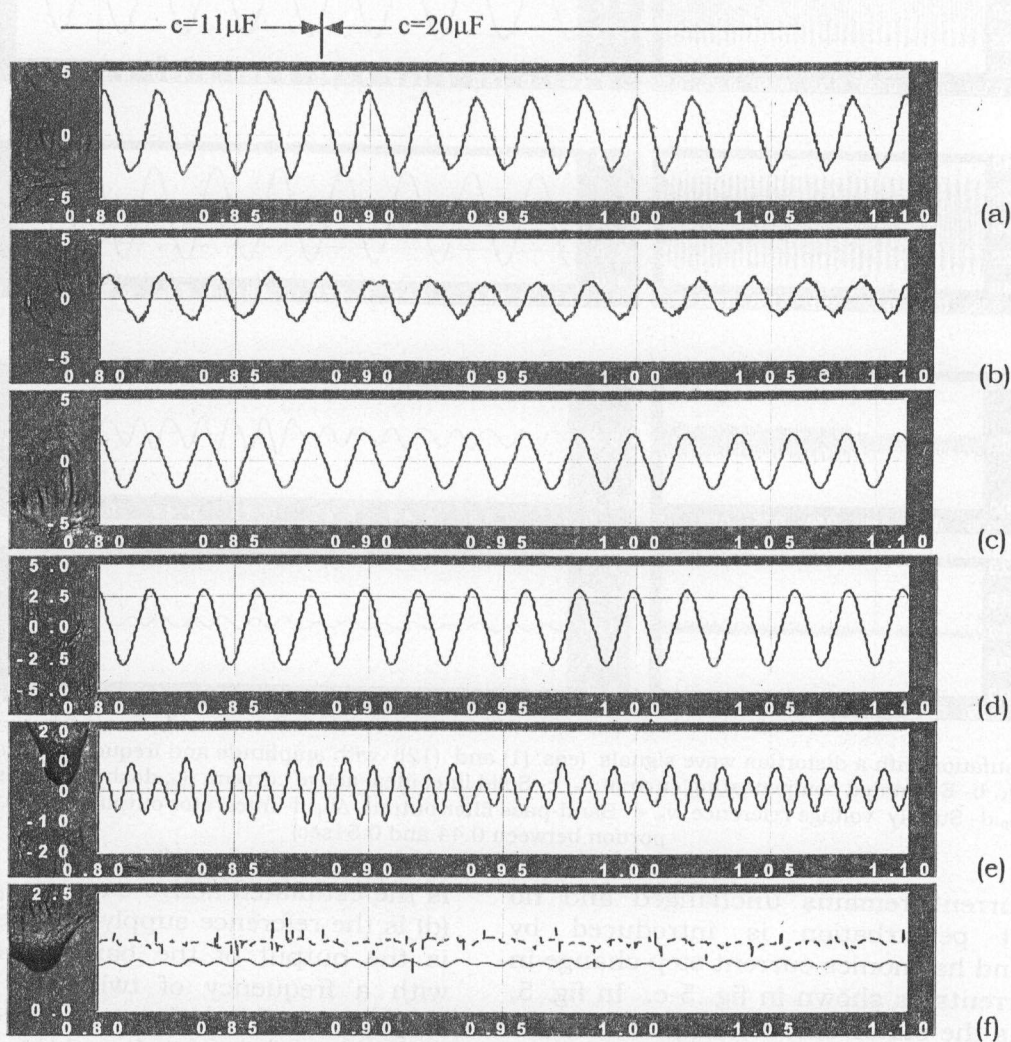


Fig. 5. Experiment for capacitor step in the controlled induction motor (50Hz). a- Stator current, i_L 0.5A/div. b- Estimated compensating current, i_c 0.5A/div. c- Estimated active current, i_{cp} 0.5A/div. d- Supply voltage reference, v_s 100v/div. e- Band-pass filter output, Δi_{ep} . f- Dashed line: motor speed 1000rpm/div; solid line: Integrator output, I_{ep} .

4. Conclusions

An adaptive estimator for detecting the instantaneous reactive and harmonic current reference has been proposed and presented. This is applicable for 1- Φ or 3- Φ active power filters and static Var compensators which allows harmonic elimination and power factor correction in nonlinear loads. Simulations and experimental results showed that, the proposed estimator requires no adjustment due to the continuously regulated closed loop action. Also, the results showed that, the estimator structure is capable of extracting compensation reference from strong disturbances efficiently, even if there are considerable frequency and amplitude variations. The estimator operates satisfactorily in the range of frequencies from about 15Hz to a limit restricted only by the frequency response of low-pass filter of DPLL and the speed of computations. This estimator, along with its simplicity, is superior to traditional open-loop systems of evaluating the compensation reference in nonlinear loads. Besides, the estimator can accurately detect and measure the active, reactive or any of its multiple harmonic current in the load. This can be achieved by adjusting, the parameters of the band-pass filter, at the start only, according to the component to be measured and multiplying the integrator output by supply voltage-phase sinusoid of that component. Finally, the ability to operate under varying frequencies makes this circuit useful for variable frequency power systems.

Appendix

-Parameters of the digital band-pass filter:

$$\beta_0 = \omega_a^2 / 2 \quad \alpha_1 = 2\sqrt{2}(\omega_a - \sqrt{2})\cos \omega_0 T_s / a,$$

$$\alpha_2 = 2(1 - \omega_a^2 + 2\cos^2 \omega_a T_s) / a,$$

$$\alpha_3 = 4(\omega_a / \sqrt{2} - 1)\cos \omega_0 T_s / a,$$

$$\alpha_4 = (\omega_a^2 + \sqrt{2}\omega_a + 1) / a.$$

Where;

$$\cos \omega_0 T_s = \frac{\cos(0.5(\omega_L + \omega_H)T_s)}{\cos(0.5(\omega_L - \omega_H)T_s)},$$

$$\omega_a = \frac{\cos \omega_0 T_s - \cos \omega_L T_s}{\sin \omega_L T_s},$$

where ω_0 , ω_L , ω_H , f_s ($1/T_s$), are center angular frequency, lower and higher cutoff angular frequencies, and sampling frequency of band-pass filter.

- Specification of IM:

$V_s=220$ V, $n_m=1340$ rpm, $I_s=1.16$ A, $r_s=35\Omega$,
 $\ell_s=0.17$ H, $r_r=2.1\Omega$, $\ell_r=0.0106$ H,
 $r_m=3400\Omega$, $\ell_m=0.99$ H, $\beta=0.00075$ N-
 m/rad/sec, $J=0.00035$ N-m/rad/sec².

- Specifications DC machine:

220V, 1.2A, 1500rpm and field voltage is 220v.

References

- [1] H. Akagi, "New trends in active filters for power conditioning," IEEE Trans. on Ind. Applications, Vol. 32 (6) (1996).
- [2] Y. Sato, T. Kawase, M. Akiyama, and T. Kataoka, "A control strategy for general-purpose active filters based on voltage detection," IEEE Trans. on Ind. Applications, Vol. 36 (5) (2000).
- [3] M. E. Abdel-Karim, "Digital signal processing for control of power converters", PhD Thesis, I.N.P.L, Nancy, France, and Faculty of Eng., Menoufia Univ, Shebin El-Kom, Egypt (Channel system) (1991).
- [4] M. E. Abdel-Karim, and A. I. Taalab, "A refined detection of a reference signal for converter controls under distortion and frequency excursion", EPE Journal, Vol. 6 (3-4) (1996).
- [5] D. Nedeljkovic, J. Nastran, D. Voncina, and V. Ambrozic, "Synchronization of active power filter current reference to the network", IEEE Trans. on Ind. Electronics, Vol. 46 (2) (1999).
- [6] L. Zhou and Z. Li, "A novel active power filter based on the least compensation current control method", IEEE Trans. on Power Electronics, Vol. 15 (4) (2000).
- [7] S. Luo. and Z. Hou, "An adaptive detecting method for harmonic and reactive

currents", IEEE Trans. on Ind. Electronics, Vol. 42 (1) (1995).

[8] P. Papamichalis, and J. So, "Implementation of fast fourier transform algorithms with TMS32020," Digital Signal Processing Applications, Taxes instruments (1988).

[9] H. Akagi, Y. Kanazawa, and A. Nabae, "Instantaneous reactive power compensators comprising switching devices without energy storage components," IEEE Trans. Ind. Applicat., Vol. IA-20 (1984).

[10] V. Soares, P. Verdelho, and G. Marques, "An instantaneous active and reactive current component method for active filters", IEEE Trans. on Power Electronics, Vol. 15 (4) (2000).

[11] S. Valiviita, and S. J. Ovaska, "Delay-less Method to generate current reference for active filters", IEEE Trans. on Ind. Electronics Vol. 45 (4) (1998).

[12] K. Chatterjee, B. G. Fernandes, and G. K. Dubey, "An instantaneous reactive volt-ampere compensator and harmonic suppressor system", IEEE Trans. on Power Electronics Vol. 14 (2) (1999).

[13] J. S. Tepper, J. W. Dixon, G. Venegas, and L. Moran, "A simple frequency-independent method for calculating the reactive and harmonic current in a nonlinear load," IEEE Trans. on Ind. Electron., Vol. 43 (6) (1996).

[14] L. Milic, U. Kamsck, and A. Jovic, "Analysis of filter bank transfer function", IEE proceeding, Vol. 134 (1) (1987).

[15] N. K. Bose, "Digital filters", University Park, Pennsylvania, North Holand (1984).

[16] J. Hejn, and J. Scott, "Z-domain model for discrete-time PLL's", IEEE trans. on Circuits and systems, Vol. (11) (1988).

[17] A. E. Lashine, S. M. R. Tahoun, and F. A. saafan, "A new approach to the speed control of wound rotor induction motors", Alexandria Engineering Journal, Vol. 38 (3), pp. B75-B85 (1999).

Received January 31, 2002
 Accepted April 29, 2002